Proceedings of the 8th World Congress on Electrical Engineering and Computer Systems and Sciences (EECSS'22)
Prague, Czech Republic - July 28- 30, 2022
Paper No. CIST 126
DOI: 10.11159/cist22.126

A Sectoral Cellular Network with Embedded Small Cells

Tsang-Ling Sheu and Yi-Hsun Lin
Department of Electrical Engineering
National Sun Yat-Sen University, Kaohsiung, Taiwan
sheu@ee.nsysu.edu.tw

Abstract **-** In this paper, we present a sectoral cellular network with embedded small cells (SCNSC). In an SCNSC network, a macro cell consists of two regions, sectors and small cells with variable radius. The system capacity in an SCNSC can be enhanced by using the fractional frequency reuse (FFR) techniques. The overall channel bandwidth is divided into two or three frequency bands depending on whether the number of sectors in a macro cell is even or odd. For the purpose of performance evaluation on the proposed SCNSC, we build an analytical model using Markov chains. Performance measures include the new-call blocking, the handoff-call dropping probabilities, and the normalized throughputs (in each sector and in its embedded small cells). By varying the speeds of mobile stations, the number of sectors, and the radius size of an embedded small cell, it is demonstrated that by adjusting either the number of sectors in a macro cell or the coverage of an embedded small cell can satisfy various service demands.

Keywords**:** sector, small cell, new-call blocking, handoff-call dropping, Markov chains

1. Introduction

Advancements in mobile wireless communication technology have led to a tremendous growth in the number of wireless devices and the volume of data transmitted. This can be achieved by combining several novel communication technologies, such as massive multiple-input multiple-output (MIMO), millimetre wave (mm-wave), and small cell deployment [1-3]. In recent decades, several schemes [4-5] have been presented to alleviate the problem of high link interruption probability due to insufficient radio resource by delaying or advancing the instant of handoff procedure. However, the previously-proposed research works have not considered the topology of a sectored macro cell with embedded several small cells.

To enhance cell coverage and data rate for a large number of users, multiple classes of BSs, macro BSs, hotspot BSs, and femtocell BSs, are installed in a heterogeneous cellular network. On the other hand, sectored antennas can be deployed to support fractional frequency reuse (FFR) in a cell to increase subscriber capacity [6]. The research works in FFR are thoroughly studied in the literatures [7-8]. Wu et al. [9] presented a three-sectored macro cell architecture with a femtocell inside each sector and a femtocell exclusion region (FER) around a macro BS. The expression of FER radius as a function of the azimuth angle relative to the macro BS was derived, which can be directly used to divide the macro cell coverage area into inner and outer regions for co-channel assignments to the macro cell and femtocells. Further from the proceeding works, Kalbkhani et al. [10] divided a macro cell into six sectors with multiple femtocells randomly installed in some sectors. According to the amount of received interferences, they presented an algorithm for channel allocation in femtocells and a closed-form formula for femtocell downlink outage probability. Tsai [11] proposed that installing three-dimension directional antenna on small cells can mitigate two-tier interference of the ultra-dense heterogeneous small-cell network and investigated the impacts of the three-dimension directional antennas and the resource block usage ratio on the system capacity and link reliability in an apartment building. Dividing a macro cell into a center zone and an edge zone (the cell coverage beyond the center zone) of three sectors, the authors in [12] aimed to mitigate interference between a macro cell and multiple femtocells in the center and edge zones by using fractional frequency reuse (FFR) under the macro cell allocating a frequency band and the femtocells selecting the sub-bands.

Although the aforementioned schemes [9-12] have improved the outage probability, including the new-call blocking and handoff-call dropping probabilities, in a macro cell with multiple small cells, they have not considered the influences of MS mobility, the coverage size of a small cell, and the number of sectors on the outage probability of a call moving from adjacent cells. Our interest in this paper is to design a sectored cellular network with small cells (SCNSC) embedded in each sector. Two region types, sectors and variable-radius small cells are classified in an SCNSC macro cell. The proposed SCNSC

can increase the system capacity by using fractional frequency reuse (FFR) since two sectors that are not adjacent can allocate the same frequency band. Each frequency band is further divided into two portions assigned to sectors and small cells, respectively. For performance evaluation, we derive the new-call blocking and handoff-call dropping probabilities, average waiting times, and normalized throughputs in each sector and its embedded small cell in terms of the call generation rate, MS moving speed, the number of sectors, and the radius size of a small cell using Markov chain theory.

The remainder of this paper is organized as follows. In Section 2, we describe the architectures of the proposed SCNSC. In Section 3, we build an analytical model by using multi-dimensional Markov chains. The analytical results and discussions are presented in Section 4. Finally, concluding remarks are given in Section 5.

2. The Proposed Scnsc

2.1. System Model

As illustrated in Figure 1, the proposed network is referred to as a sectoral cellular network with embedded small cells (SCNSC). In the SCNSC, a macro cell consists of two region types, sectors and small cells with variable radius. Coverage of the macro cell is sectored by using multi-directional antennas and a small cell with variable-radius is embedded within each sector. We assume that the maximum coverage of a small cell is an inscribed circle within a sector. Additionally, we assume that the coverage of a small cell spanning the boundary of two sectors is not allowable.

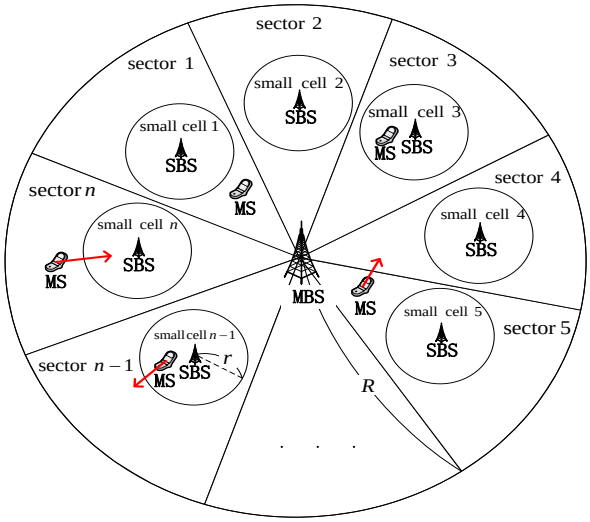

Figure 1. System architecture of the SCNSC.

We summarize the symbols and denotations for the SCNSC in Table 1. Let n be the number of sectors for a macro cell. R and r, respectively, represent the radiuses of a macro cell and a small cell. Ar is defined as the ratio of a small cell coverage to a sector region, as expressed in Equation (1). The system capacity is enhanced by using FFR. Therefore, the overall channel bandwidth is divided into n_f frequency bands, where n_f is two (three) if n is even (odd).

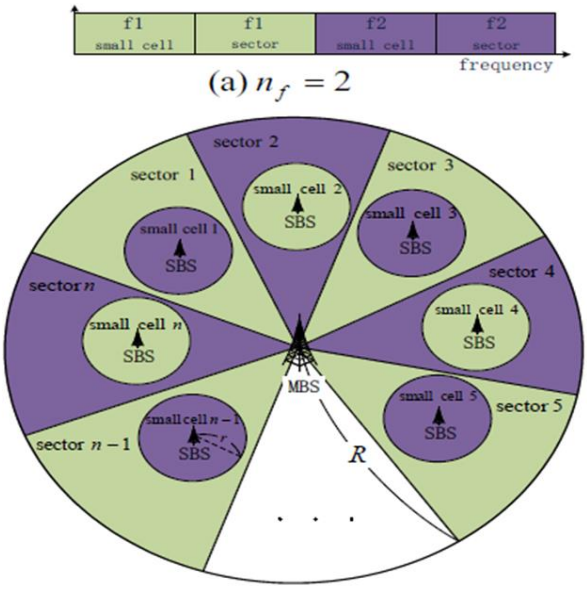

(b) Frequency utilization map

Figure 2. Channel allocations when n is even.

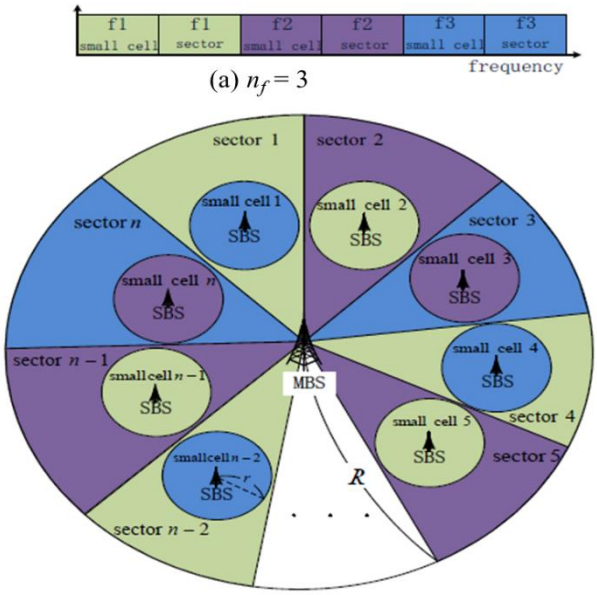

(b) Frequency utilization map

Figure 3. Channel allocations when n is odd.

Figure 2 shows channel allocation for the system when n is even. As shown in Figure 2(a), the system bandwidth is divided into two frequency bands in different colors and each frequency band is composed of two portions, one is for small cells and the other is for sectors. As illustrated in Figure 2(b), in order to reduce co-channel interference, two adjacent sectors allocate different frequency bands and the two embedded small cells use different frequency bands from their respective sectors. Similarly, Figure 3 shows channel allocation for the system when n is odd. Let *N* denote the total number of channels, i.e.,

time slots, frequency carriers, or time-and-frequency blocks, in the system. N_{sr} (N_{sc}) is the total number of available channels in the same frequency band for a sector (small cell) region. There are two kinds of new calls (NCs), initiating in a sector region or a small cell coverage, designated by NC_{sr} and NC_{sc}, respectively. Three kinds of handoff calls (HCs) are generated. One is from those MSs moving from a sector region to its embedded small cell, denoted as HC_{sr_sc}. The second one is from those MSs moving in the reverse direction, denoted as HC_{sc_sr}. The third one is from those MSs moving between two sectors, denoted as HC_{sr_sr}.

$$Ar = \frac{\pi r^2}{\pi R^2 / n} = \frac{nr^2}{R^2} \tag{1}$$

Table 1. Symbols and Denotations

Symbols	Denotations
n	the number of sectors for a macro cell
R	the radius of a macro cell (in meters)
r	the radius of a small cell (in meters)
Ar	a small cell coverage divided by to a sector region
n_f	the number of frequency bands
N	the total number of channels in the system
N_{sr}	the total number of available channels in a sector
N_{sc}	the total number of available channels in a small cell
NC_{sr}	new calls initiating in a sector
NC_{sc}	new calls initiating in a small cell
HC_{sr_sr}	handoff calls of MSs moving between two sectors
HC_{sr_sc}	handoff calls of MSs moving from a sector to its embedded small cell
HC_{sc_sr}	handoff calls of MSs moving from a small cell to its associated sector

2.2. Handoff Rates

There are three kinds of handoff calls (designated by HC_{sc_sr}, HC_{sr_sc}, and HC_{sr_sr}) in the SCNSC. Referring to the works [28-29], Equation (2) expresses the probability of an MS moving from a small cell area to its associated sector, and vice versa.

$$\frac{E[V] \times L}{\pi \times A} \tag{2}$$

where L is the length of the boundary between a small cell and a sector, $E[V]$ is the average moving speed of an MS, and A is the coverage area of a small cell or sector. As illustrated in Figure 4, three kinds of handoff rate are derived as follows.

Let ω_{sc_sr} , as shown in Equation (3), denote the handoff rate of HC_{sc_sr}. L and A in Euqation (2) are equal to $2\pi r$ and πr^2, respectively. Then,

$$\omega_{sc\_sr} = \frac{E[V]\times(2\pi r)}{\pi\times(\pi r^2)} = \frac{2\times E[V]}{\pi\times r} \tag{3}$$

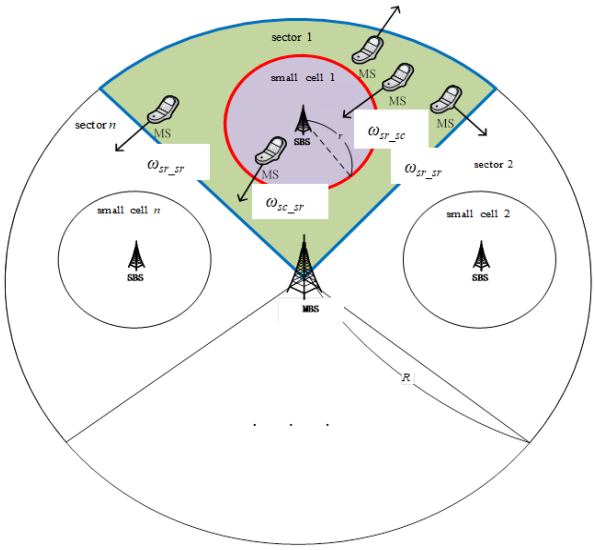

Figure 4. Three kinds of handoff calls.

Let ω_{sr_sc} , as shown in Equation (4), denote the handoff rate of HC_{sr_sc}. Similarly, L and A in Equation (2) are equal to $2\pi r$ and $\pi R^2/n - \pi r^2$, respectively. Then,

$$\omega_{sr\_sc} = \frac{E[V]\times(2\pi r)}{\pi\times(\pi R^2/n - \pi r^2)} = \frac{2\times E[V]\times r\times n}{\pi\times(R^2 - n\times r^2)} \tag{4}$$

Let ω_{sr_sr} denote the handoff rate of HC_{sr_sr}. L represents the boundary of a sector, which is equal to $2R + 2\pi R/n$. However, HC_{sr_sr} is defined as a handoff call when an MS moves from a sector to two adjacent sectors without including an MS moving out of the macro cell. Thus, L in Equation (2) is modified as expressed in Equation (5). Replacing A and L in Equation (2) with the formulas for the kind of handoff, we obtain Equation (6).

$$L = (2R + 2\pi R/n)\times(R/(2R + 2\pi R/n)) \tag{5}$$

$$\omega_{sr\_sr} = \frac{E[V]\times(2R + 2\pi R/n)}{\pi\times(\pi R^2/n - \pi r^2)}\times\frac{R}{2R + 2\pi R/n} = \frac{E[V]\times R\times n}{\pi^2\times(R^2 - n\times r^2)} \tag{6}$$

3. THE MATHEMATICAL MODELS

To analyze the performance of the proposed SCNSC, we build a mathematical model using Markov chains. If n is even, each state of the transition matrix is defined as a four-dimensional vector, denoted as [i, j, x, y], in which i (j) is the number of calls in the odd (even)-indexed sector and x (y) is the number of calls in the odd (even)-indexed small cell. On the other hand, if n is odd, each state of the transition matrix is defined as a six-dimensional vector, denoted as [i, j, k, x, y, z], in which i (j or k) is the number of calls in the sector indexed by a multiple of three plus one (two or zero) and x (y or z) is the number of calls in the small cell indexed by a multiple of three plus one (two or zero). Firstly, we calculate the transition rates, which contain the arrival and departure rates between any two of the states. Then, each state probability is obtained and the performance measures, including the NC blocking and HC dropping probabilities, the average waiting time, and the normalized throughput,

are derived in terms of the obtained state probabilities. We assume MSs are homogeneously distributed in a macro cell. Each new/handoff call occupies one channel. The average moving speed of MSs in either of a sector or a small cell is the same.

The bandwidth is channelized with a maximum number, denoted as N. Under the above assumptions, the number of available channels in the same frequency band for a small cell, denoted as N_{sc}, can be expressed by Equation (7). Moreover, the number of available channels in the same frequency band for a sector region excluding its embedded cell coverage, denoted as N_{sr}, is expressed as Equation (8).

$$N_{sc} = \frac{N}{n_f} \times Ar \tag{7}$$

$$N_{sr} = \frac{N}{n_f} \times (1 - Ar) \tag{8}$$

3.1. Handoff Rates

The transition rates in the Markov model include arrival rate, denoted by λ, and departure rate, denoted by μ. The arrival rate is composes of those from NCs and HCs, while the departure rate is generated from call handoff or termination. The arrival rates associated with NCs, consisting of NC_{sc} and NC_{sr}, are denoted as λ_{sc} and λ_{sr}, respectively. The arrival rates from HCs, consisting of HC_{sr_sr}, HC_{sr_sc}, and HC_{sc_sr}, are denoted by λ_{sr_sr}, λ_{sr_sc} , and λ_{sc_sr}, respectively. Similarly, the departure rates caused by call handoff, consisting of HC_{sr_sr}, HC_{sr_sc}, and HC_{sc_sr}, are denoted as μ_{sr_sr}, μ_{sr_sc} , and μ_{sc_sr}, respectively. The departure rates caused by call termination include μ_{sc} and μ_{sr}, which stand for the calls terminating in a small cell and a sector region, respectively. μ_{sc} contains two parts: one, denoted as μ_{sc_t}, is for NCc originally initiating in a small cell and the other, denoted as $\mu_{sr\_sc\_t}$, is for HC_{sr_sc} terminating in a small cell. μ_{sr} contains three parts: one, denoted as μ_{sr_t}, is for NCs originally initiating in a sector and the other two, denoted as $\mu_{sc\_sr\_t}$, and $\mu_{sr\_sr\_t}$, respectively for HC_{sc_sr} and HC_{sr_sr} terminating in a sector. Table 2 summarizes the abovementioned transition rates in the Markov model.

Therefore, λ_{sc} and λ_{sr} can be expressed by Equations (9) and (10), respectively. In the balanced condition of the Markov model, the arrival rate and departure rate caused by call handoff is the same. That's, λ_{sr_sr}, λ_{sr_sc}, and λ_{sc_sr} are equal to μ_{sr_sr}, μ_{sr_sc}, and μ_{sc_sr}, respectively. We can obtain the handoff-call arrival (departure) rate for each state by multiplying the varied element in the state by the associated handoff rate, as derived in Section 2.2. As to the departure rate caused by call termination in a small cell coverage (μ_{sc}) is the sum of μ_{sc_t} and $\mu_{sr\_sc\_t}$, which are expressed by Equations (11) and (12), respectively. Similarly, the departure rate caused by call termination in a sector region (μ_{sr}) is the sum of μ_{sr_t}, $\mu_{sc\_sr\_t}$, and $\mu_{sr\_sr\_t}$, which are expressed in Equations (13), (14), and (15), listed one by one below.

$$\lambda_{sc} = \lambda \times Ar \tag{9}$$

$$\lambda_{sr} = \lambda \times (1 - Ar) \tag{10}$$

$$\mu_{sc\_t} = \mu \times Ar \times \frac{\lambda_{sc}}{\lambda_{sc} + \lambda_{sr\_sc}} \tag{11}$$

$$\mu_{sr\_sc\_t} = \mu \times Ar \times \left(1 - \frac{\lambda_{sc}}{\lambda_{sc} + \lambda_{sr\_sc}}\right) \tag{12}$$

$$\mu_{sr\_t} = \mu \times (1 - Ar) \times \frac{\lambda_{sr}}{\lambda_{sr} + \lambda_{sc\_sr} + 2 \times \lambda_{sr\_sr}} \tag{13}$$

$$\mu_{sc\_sr\_t} = \mu \times (1 - Ar) \times \frac{\lambda_{sc\_sr}}{\lambda_{sr} + \lambda_{sc\_sr} + 2 \times \lambda_{sr\_sr}} \tag{14}$$

$$\mu_{sr\_sr\_t} = \mu \times (1 - Ar) \times \frac{2 \times \lambda_{sr\_sr}}{\lambda_{sr} + \lambda_{sc\_sr} + 2 \times \lambda_{sr\_sr}} \tag{15}$$

3.2. Markovian States

All of the states in the Markov model are composed of the following five portions:

(a) The number of calls in either a small cell or a sector does not exceed the upper limit. That's, each sector-related (small-cell-related) element of a state varies from 0 to N_{sr} (N_{sc}) and there are n_f frequency bands. Therefore, the total number of states in this portion, denoted as N_1, is calculated as in Equation (16).

$$N_1 = (N_{sr} + 1)^{n_f} \times (N_{sc} + 1)^{n_f} \tag{16}$$

(b) NC in a small cell being blocked: when the number of calls in a small cell reaches the maximum value, i,e., N_{sc}, an NC will be blocked. The total number of states in the portion, denoted as N_2, is calculated as in Equation (17).

$$N_2 = (N_{sr} + 1)^{n_f} \times (N_{sc} + 1)^{n_f - 1} \times n_f \tag{17}$$

(c) NC in a sector being blocked: when the number of calls in a sector reaches the maximum value, i,e., N_{sr}, an NC will be blocked. The total number of states in the portion, denoted as N_3, is calculated as in Equation (18).

$$N_3 = (N_{sr} + 1)^{n_f - 1} \times (N_{sc} + 1)^{n_f} \times n_f \tag{18}$$

(d) HC moving into a small cell being dropped: when the number of calls in a small cell reaches the maximum value (N_{sc}), an HC will be dropped. The total number of states in the portion, denoted as N_4, is calculated as in Equation (19).

$$N_4 = N_{sr} \times (N_{sr} + 1)^{n_f - 1} \times (N_{sc} + 1)^{n_f - 1} \times n_f \tag{19}$$

(e) HC moving into a sector being dropped: there are two situations in the portion of states. That's, an HC is moving from a small cell to a sector and an HC is moving from a sector to two adjacent sectors. The total number of states in the portion, denoted as N_5, is calculated as in Equation (20) depending on the number of sectors (denoted by n), is even or odd.

$$N_5 = \begin{cases} (N_{sr} + 1)^{n_f - 1} \times (N_{sc} + 1)^{n_f - 1} \times N_{sc} \times n_f \\ + N_{sr} \times (N_{sc} + 1)^{n_f} \times n_f \\ - (N_{sc} + 1) \times N_{sc} \times N_{sr} \times n_f, \text{ if } n \text{ is even} \\ \\ (N_{sr} + 1)^{n_f - 1} \times (N_{sc} + 1)^{n_f - 1} \times N_{sc} \times n_f \\ + (N_{sr} \times 2(N_{sr} + 1) - N_{sr}^2) \times (N_{sc} + 1)^{n_f} \times n_f \\ - (N_{sc} + 1)^{n_f - 1} \times ((N_{sr} + 1)^{n_f - 1} - 1) \times n_f, \text{ if } n \text{ is odd} \end{cases} \tag{20}$$

By summing Equations (16) to (20), we can obtain the total number of the states, N_t, as expressed in Equation (21). The size of the transition matrix for the Markov model is N_t xN_t.

$$N_t = N_1 + N_2 + N_3 + N_4 + N_5 \tag{21}$$

3.3. Performance Measures

An NC may get rejected in a small cell if one of the small-cell-related elements in the current state is N_{sc} and one more NC makes the element become N_{sc} +1. Thus, the NC blocking probability in a small cell, denoted as Pb_{sc}, is expressed as Equation (22). Similarly, an NC may get rejected in a sector if one of the sector-related elements in the current state is N_{sr}. Thus, the NC blocking probability in a sector, denoted as Pb_{sr}, is expressed by Equation (23).

$$Pb_{sc} = \begin{cases} \sum_{i=0}^{N_{sr}} \sum_{j=0}^{N_{sr}} \sum_{y=0}^{N_{sc}} P(i, j, N_{sc}+1, y) \times n_f, \text{ if } n \text{ is even} \\ \sum_{i=0}^{N_{sr}} \sum_{j=0}^{N_{sr}} \sum_{k=0}^{N_{sr}} \sum_{y=0}^{N_{sc}} \sum_{z=0}^{N_{sc}} P(i, j, k, N_{sc}+1, y, z) \times n_f, \text{ if } n \text{ is odd} \end{cases} \quad (22)$$

$$Pb_{sr} = \begin{cases} \sum_{j=0}^{N_{sr}} \sum_{x=0}^{N_{sc}} \sum_{y=0}^{N_{sc}} P(N_{sr}+1, j, x, y) \times n_f, \text{ if } n \text{ is even} \\ \sum_{j=0}^{N_{sr}} \sum_{k=0}^{N_{sr}} \sum_{x=0}^{N_{sc}} \sum_{y=0}^{N_{sc}} \sum_{z=0}^{N_{sc}} P(N_{sr}+1, j, k, x, y, z) \times n_f, \text{ if } n \text{ is odd} \end{cases} \quad (23)$$

On the other hand, an HC moving from a sector to a small cell gets no services when one of the small-cell-related elements in the current state reaches N_{sc}. one more HC makes the element become $(N_{sc}+1)'$. We use the symbol prime to indicate the case when the arriving call belongs to HCs. Therefore, the HC dropping probability for MSs moving from a sector to a small cell, denoted by Pd_{sr_sc}, is calculated as Equation (24).

$$Pd_{sr\_sc} = \begin{cases} \sum_{i=0}^{N_{sr}} \sum_{j=0}^{N_{sr}} \sum_{y=0}^{N_{sc}} P(i, j, (N_{sc}+1)', y) \times n_f, \text{ if } n \text{ is even} \\ \sum_{i=0}^{N_{sr}} \sum_{j=0}^{N_{sr}} \sum_{k=0}^{N_{sr}} \sum_{y=0}^{N_{sc}} \sum_{z=0}^{N_{sc}} P(i, j, k, (N_{sc}+1)', y, z) \times n_f, \text{ if } n \text{ is odd} \end{cases} \quad (24)$$

We define the normalized throughput (NT) as the individual channel utilization for a sector, a small cell, or a macro cell. Let Γ_{sr} be the NT for a sector. As expressed in Equation (25), Γ_{sr} consists of three conditions: one is for the states the channels are available for both in a sector and a small cell (i.e., the first term of Eq. (25)); one is for the states the channels are fully occupied in a sector and an NC or HC gets no services in a sector (i.e., the second and third terms of Eq. (25)); the other one is for the states the channels are fully occupied in a small cell and an NC or HC gets no services in a small cell (i.e., the fourth and fifth terms of Eq. (25)). Similar to the derivation of Γ_{sr}, we can obtain the NT for a small cell, denoted as Γ_{sc}. Finally, let Γ_{mc} be the NT for the macro cell. Similarly, we can derive Γ_{mc}. Equations of Γ_{sr} and Γ_{mc} are omitted here due to the page length.

$$
\Gamma_{sr} = \begin{cases}
\sum_{i=0}^{N_{sr}} \sum_{j=0}^{N_{sr}} \sum_{x=0}^{N_{sc}} \sum_{y=0}^{N_{sc}} \frac{i+j}{N_{sr} \times n_f} \times P(i, j, x, y) \\
+[\sum_{j=0}^{N_{sr}} \sum_{x=0}^{N_{sc}} \sum_{y=0}^{N_{sc}} \frac{N_{sr}+j}{N_{sr} \times n_f} \times P(N_{sr}+1, j, x, y) \\
+\sum_{j=0}^{N_{sr}} \sum_{x=0}^{N_{sc}} \sum_{y=0}^{N_{sc}} \frac{N_{sr}+j}{N_{sr} \times n_f} \times P((N_{sr}+1)', j, x, y)] \times n_f \\
+[\sum_{i=0}^{N_{sr}} \sum_{j=0}^{N_{sr}} \sum_{y=0}^{N_{sc}} \frac{i+j}{N_{sr} \times n_f} \times P(i, j, N_{sc}+1, y) \\
+\sum_{i=0}^{N_{sr}} \sum_{j=0}^{N_{sr}} \sum_{y=0}^{N_{sc}} \frac{i+j}{N_{sr} \times n_f} \times P(i, j, (N_{sc}+1)', y)] \times n_f, \text{ if } n \text{ is even} \\
\\
\sum_{i=0}^{N_{sr}} \sum_{j=0}^{N_{sr}} \sum_{k=0}^{N_{sr}} \sum_{x=0}^{N_{sc}} \sum_{y=0}^{N_{sc}} \sum_{z=0}^{N_{sc}} \frac{i+j+k}{N_{sr} \times n_f} \times P(i, j, k, x, y, z) \\
+[\sum_{j=0}^{N_{sr}} \sum_{k=0}^{N_{sr}} \sum_{x=0}^{N_{sc}} \sum_{y=0}^{N_{sc}} \sum_{z=0}^{N_{sc}} \frac{N_{sr}+j+k}{N_{sr} \times n_f} \times P(N_{sr}+1, j, k, x, y, z) \\
+\sum_{j=0}^{N_{sr}} \sum_{k=0}^{N_{sr}} \sum_{x=0}^{N_{sc}} \sum_{y=0}^{N_{sc}} \sum_{z=0}^{N_{sc}} \frac{N_{sr}+j+k}{N_{sr} \times n_f} \times P((N_{sr}+1)', j, k, x, y, z)] \times n_f \\
+[\sum_{j=0}^{N_{sr}} \sum_{k=0}^{N_{sr}} \sum_{x=0}^{N_{sc}} \sum_{y=0}^{N_{sc}} \sum_{z=0}^{N_{sc}} \frac{i+j+k}{N_{sr} \times n_f} \times P(i, j, k, N_{sc}+1, y, z) \\
+\sum_{j=0}^{N_{sr}} \sum_{k=0}^{N_{sr}} \sum_{x=0}^{N_{sc}} \sum_{y=0}^{N_{sc}} \sum_{z=0}^{N_{sc}} \frac{i+j+k}{N_{sr} \times n_f} \times P(i, j, k, (N_{sc}+1)', y, z)] \times n_f, \text{ if } n \text{ is odd}
\end{cases} \tag{25}
$$

4. Analytical Results

4.1. Parameters and Settings

We evaluate the system performance of our proposed SCNSC via the analytical model built in Section 3. By setting the parameters as shown in Table 2, the transmission radius of the macro cell is fixed at 1000 meters and the transmission radius of a small cell is varied to change its coverage. The total number of channels in the system is given by 60 and the number of sectors is set to 3 and 6. In order to observe the effect of the average moving speed ($E[V]$) of MSs on the new call (NC) blocking probability and the handoff call (HC) dropping probability, the average moving speed, $E[V]$, are set to 20, 40, and 60 km/hr. The arrival rate of NCs varies from 0.001 to 0.006 and the departure rate of NCs is fixed at 0.005. The total number of MSs in the macro cell is assumed to be 200. The corresponding transition matrix and the associated transition rates between any two states can be computed. All of the state probabilities are calculated by running the mathematical tool on MATLAB.

Table 2. Parameters and their Values

Parameters	Values
R	1000 meters
r	50, 150, 250 meters
N	60
n	3, 6
$E[V]$	20, 40, 60 km/hr
λ	0.001~0.006
μ	0.005

4.2. Numerical Results

The numerical simulation results are presented from Figures 5 to 12. By fixing the radius of a small cell (r) at a medium size (150 meters), Figures 5 to 12 show the performance measures derived versus different traffic loads. In Figures 5 and 6, it is observed that the NC blocking probabilities in a sector and a small cell, Pb_{sr} and Pb_{sc}, both increase with the system traffic load and the average moving speeds of MSs, since the increment in traffic load or MS moving speed results in more NCs and HCs. Besides, it is found that the number of sectors (n) has opposing influences on Pb_{sr} and Pb_{sc}. Since the greater n is, the less the sector region, Pb_{sr} increases with n due to more channels being occupied by handoff calls. On the contrary, Pb_{sc} for n = 6 is lower than that for n = 3 because an even number of sectors (e.g., n = 6) has more channels allocated for a small cell than an odd number of sectors (e.g., n = 3).

Figures 7, 8, and 9, respectively, show the HC dropping probabilities, Pb_{sr_sr} (handoff from a small cell to another small cell), Pb_{sc_sr} (handoff from a sector to a small cell), and Pb_{sr_sc} (handoff from a small cell to a sector). By fixing the radius of a small cell to 150 meters, three phenomenon observed from Figures 7 to 9 are worthy to notice. First, the three HC dropping probabilities always declines when the traffic load reaches a certain level. This is because although larger traffic load means more NCs initiating in the system, yet since the number of HCs remains the same, the latter may get services much easier due to the increasing blocking rates of NCs. Second, smaller number of sectors ($n=3$) has relatively lower handoff dropping probabilities than a larger number of sector ($n=6$). Third, lower moving speed (E[V]=20 km/hr) of MS has relatively lower handoff dropping probabilities than MS of higher moving speed (E[V]=60 km/hr). Obviously, the reasons of the last two phenomenon may look quite straightforward. However, from Figure 9, we observe one adverse phenomenon. That is, in the case of handoff calls moving from a small cell to a sector, smaller number of sectors ($n=3$) received much higher handoff dropping probabilities than a larger number of sectors ($n=6$). It is noticed that when the number of sectors is increased, the coverage area of a sector becomes smaller and it is almost equal to the area of a small cell. Therefore, handoff from a small cell to a sector is unlikely to happen. Consequently, the handoff call dropping probabilities from a small cell to a sector for a larger number of sectors ($n=6$) is relatively smaller than that for a smaller number of sector ($n=3$).

As to the normalized throughput, the simulation results are plotted in Figures 10, 11, and 12. By fixing the MS moving speed to E[V]=40 km/hr, first, we can observe that a larger number of sector ($n=6$) and a smaller radius of a small cell (r = 50 meters) can achieve the highest normalized throughput. This is because a larger number of sectors results in a smaller coverage of a sector and a smaller radius results in a smaller coverage of a small cell. As a result, a larger number of handoff calls may become much easier to move from a small cell to its associated sector. From Figure 9, we have noticed that under these two conditions the dropping probabilities for the handoff calls moving from a small cell to a sector is quite low. Hence, the normalized throughput can be increased when a larger number of sectors and a smaller coverage of an embedded small cell are deployed.

At last, from Figure 12, it is demonstrated that using the fractional frequency reuse (FFR) techniques in a sectored cellular network can greatly improve the system capacity, even though the traffic load is increased to near 0.8. Additionally, we observe that the normalized throughput of the macro cell (Γmc) for $n=6$ is relatively larger than that for $n=3$ no matter the size (either r = 50 or r = 150 meters) of an embedded small cell is. Again, from Figure 12, we notice that for a larger sector number ($n=6$) and a smaller coverage of a small cell (r = 50 meters), a macro cell may exhibit the highest normalized throughput when the MS moving speed (E[V]) is equal to 40 km/hr.

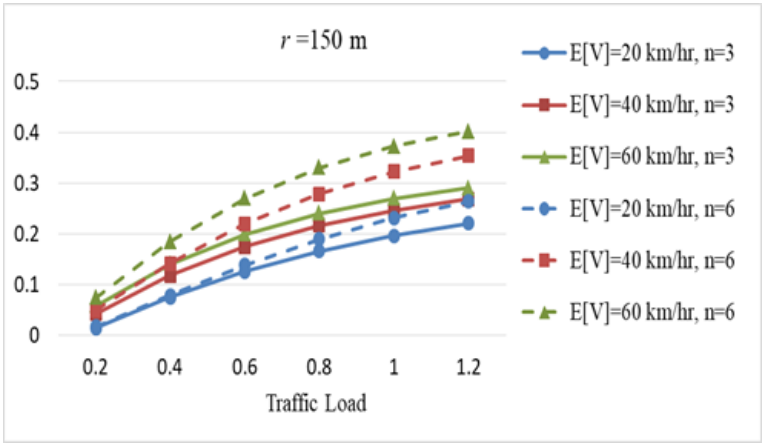

Figure 5. The NC blocking probability versus traffic load
(Pbsr, for a sector)

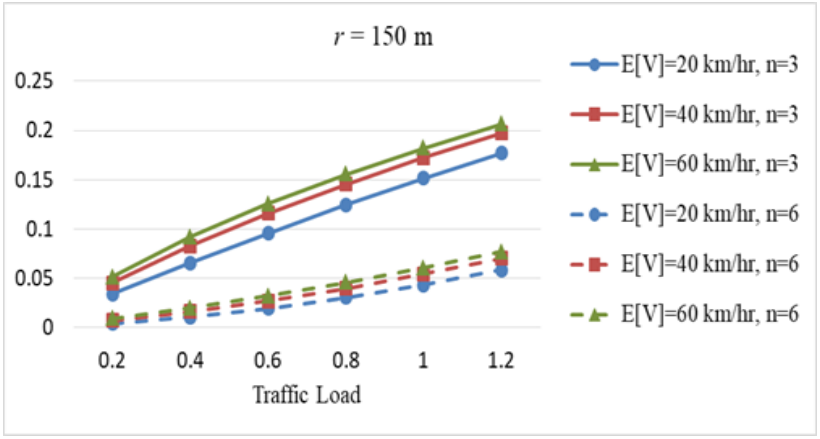

Figure 6. The NC blocking probability versus traffic load
(Pbsc, for a small cell)

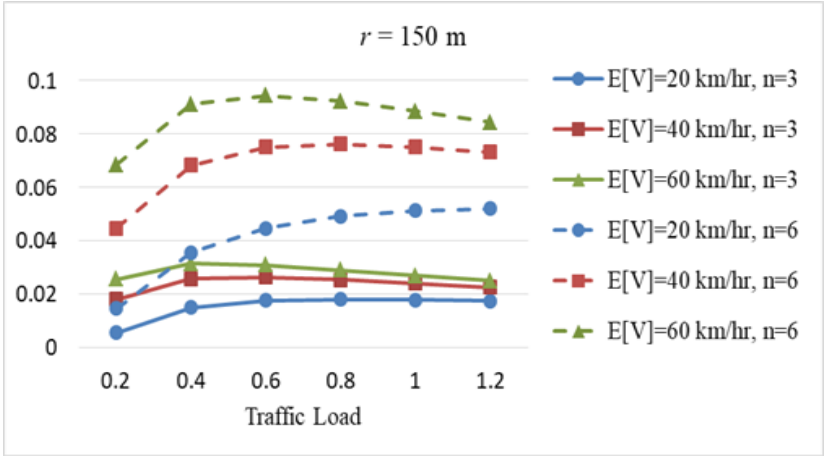

Figure 7. The HC dropping probability versus traffic load
(Pbsr_sr, handoff from a small cell to another small cell)

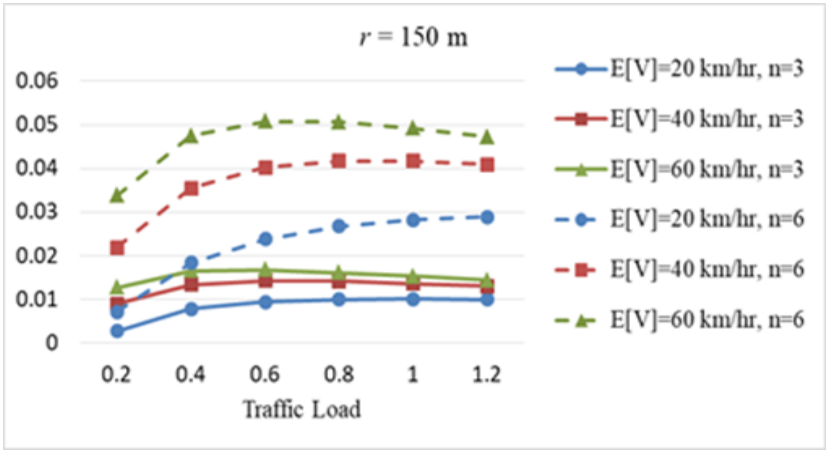

Figure 8. The HC dropping probability versus traffic load
(Pbsc_sr, handoff from a sector to a small cell)

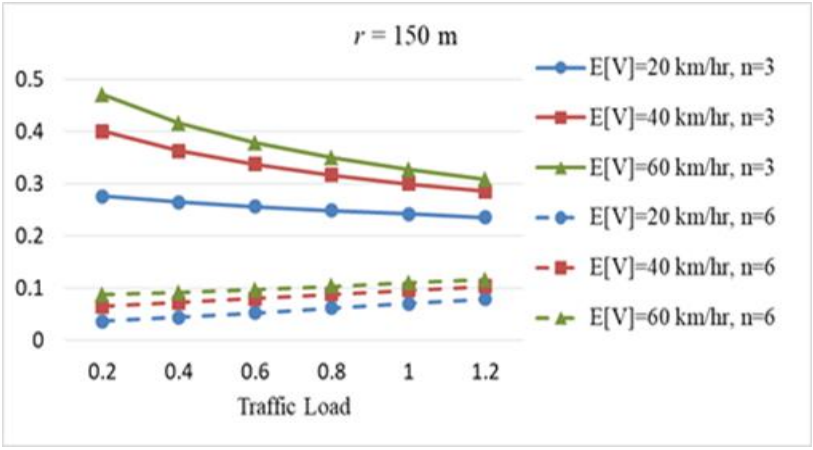

Figure 9. The HC dropping probability versus traffic load
(Pbsr_sc, handoff from a small cell to a sector)

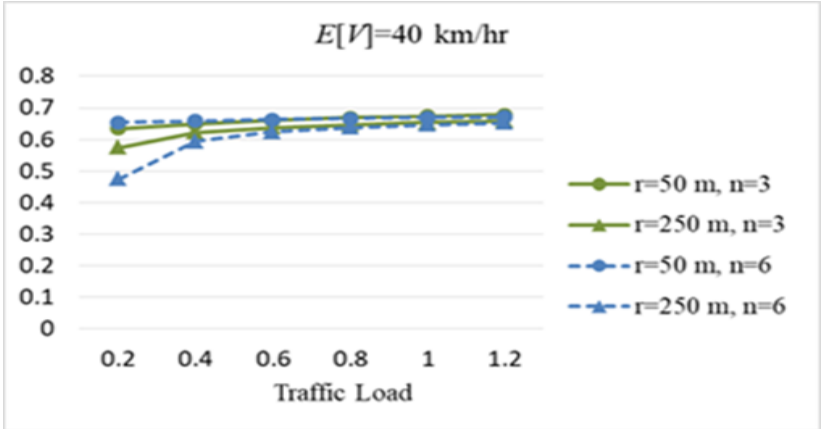

Figure 10. The normalized throughput versus traffic load
(Γsr, for a small cell)

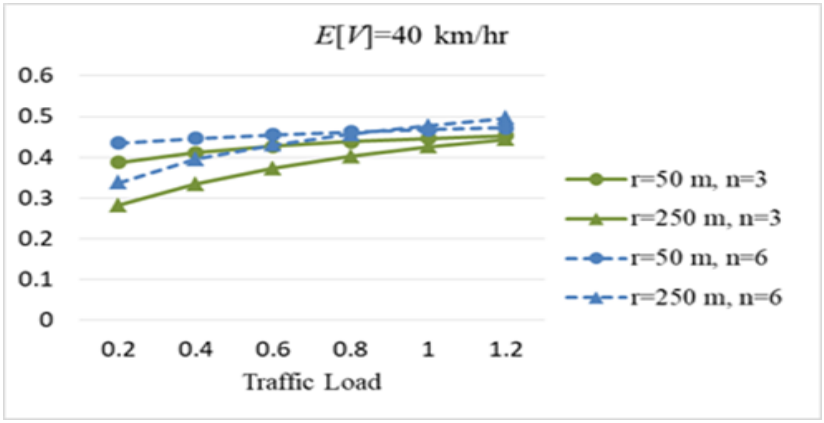

Figure 11. The normalized throughput versus traffic load
(Γsc, for a sector)

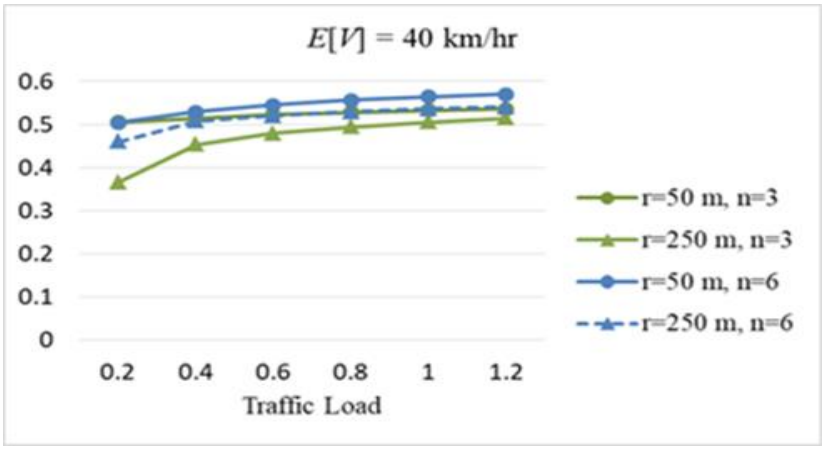

Figure 12. The normalized throughput versus traffic load
(*Γmc*, for a macro cell)

5. Conclusion

We have presented an architecture of a sectoral cellular network with embedded small cells (SCNSC). In the SCNSC, a multi-dimensional antenna is used for sectoring a macro cell and each sector is embedded with a small cell to support the huge amounts of data transmitted through hot spots and to increase the cell coverage. The overall system capacity is enhanced by using FFR techniques. On the proposed SCNCS, we built an analytical model by using Markov chains to evaluate the system performance. The performance measures, including new-call blocking and handoff-call dropping probabilities, and the normalized throughputs for a macro cell, the sector, and the embedded small cell. From the analytical results, we have demonstrated that the new-call blocking and handoff-call dropping probabilities in a small cell can be reduced significantly by increasing the number of sectors and by decreasing the radius of a small cell. On the contrary, the handoff-call dropping probability in a sector can be decreased by decreasing both the number of sectors and the radius of a small cell. To maximize the normalized throughput of the proposed SCNSC system, we can increase the number of sectors and decrease the portion of small cell coverage within a sector region. In summary, one of the contributions revealed by this paper is that one can adjust either the number of sectors or the coverage of an embedded small cell to satisfy different service demands.

Acknowledgements

This work was supported by the Ministry of Science and Technology, Taiwan, under the grant no. MOST 110-2221-E-110-009. The authors thank the anonymous reviewers.

References

[1] J. Chen, X. Ge, and Q. Ni, “Coverage and Handoff Analysis of 5G Fractal Small Cell Networks,” IEEE Transactions on Wireless Communications, vol. 18, no. 2, pp.1263-1276, Feb. 2019.

[2] M. Agiwal, A. Roy, and N. Saxena, “Next Generation 5G Wireless Networks: A Comprehensive Survey,” IEEE Communications Surveys & Tutorials, vol. 18, no. 3, pp. 1617-1655, 3rd Quarter, 2016.

[3] A. Orsino, W. Guo, and G. Araniti, “5G Multiscale Mobility : A Look at Current and Upcoming Models in the Next Technology Era,” IEEE Vehicular Technology Magazine , vol. 13, no. 1, pp. 120-129, Mar. 2018.

[4] H. Jiang, Z. Xiao, Z. Li, J. Xu, F. Zeng, and D. Wang, "An Energy-Efficient Framework for Internet of Things Underlaying Heterogeneous Small Cell Networks," in IEEE Transactions on Mobile Computing, June 2020, doi: 10.1109/TMC.2020.3005908.

[5] S. Elhoushy and W. Hamouda, "Performance of Distributed Massive MIMO and Small-Cell Systems Under Hardware and Channel Impairments," in IEEE Transactions on Vehicular Technology, vol. 69, no. 8, pp. 8627-8642, Aug. 2020, doi: 10.1109/TVT.2020.2998405.

[6] V. V. Paranthaman, G. Mapp, P. Shah, H. X. Nguyen, and A. Ghos, “Exploring Markov Models for the Allocation of Resources for Proactive Handover in a Mobile Environment,” 40th IEEE Local Computer Networks Conference Workshops, pp. 26-29, Clearwater Beach, Florida, USA, 26-29, Oct. 2015.

[7] S. Y. Kim, S. Ryu, C. H. Cho, and H. W. Lee, “Performance analysis of a cellular network using frequency reuse partitioning,” International Journal on Performance Evaluation, vol. 70, no. 2, pp. 77-89, Feb. 2013.

[8] S. Sezginer and H. Sari, “Full Frequency Reuse in OFDMA-Based Wireless Networks with Sectored Cells,” 2009 IEEE Wireless Communications and Networking Conference, Budapest, Hungary, 5-8 April, 2009.

[9] J. Wu et. al., “Femtocell Exclusion Regions in Hierarchical 3-sector Macrocells for Co-channel Deployments,” 1st IEEE International Conference on Communications in China, pp. 541-545, Beijing, China, 15-17, Aug. 2012.

[10] H. Kalbkhani et. al., “Outage Probability of Femtocells in Two-tier Networks with 6-sector Macrocells,” 6th International Symposium on Telecommunications, pp. 283-288, Tehran, Iran, 6-8, Nov. 2012.

[11] Ang-Hsun Tsai, “Two-Tier Interference Mitigation with Directional Antennas for Small-Cells in an Apartment Building,” 15th International Symposium on Wireless Communication Systems, Lisbon, Portugal, 28-31, Aug. 2018.

[12] D. López-Pérez, H. Claussen, and L. Ho, “The Sector Offset Configuration Concept and its Applicability to Heterogeneous Cellular Networks,” IEEE Communications Magazine, vol. 53, no. no. 3, pp. 190-198, Mar. 2015.